Desalination and Water Treatment
www.deswater.com
doi: 10.1080/19443994.2014.940395

56 (2015) 792–805
October

Taylor & Francis
Taylor & Francis Group

Modeling of two up-flow fixed-bed columns in series for the biosorption of Cr^{6+} and Ni^{2+} by sugarcane bagasse

Iván L. Rodríguez Rico[a], Nabin Kumar Karna[a], Inés Alomá Vicente[a], Roberto Cabrera Carrazana[a], Alicia Ronda[b,*]

[a]*Chemical Engineering Department, Central University "Marta Abreu" of Las Villas, Carretera a Camajuaní Km 5 1/2, Santa Clara, Villa Clara, Cuba, Tel. +53 42 211825; emails: ivanl@uclv.edu.cu (I.L. Rodríguez Rico), kumark@uclv.edu.cu (N.K. Karna), Tel. +53 42 226768; email: inesav@uclv.edu.cu (I.A. Vicente), Tel. +53 42 219650; email: rcabrera@uclv.edu.cu (R.C. Carrazana)*

[b]*Chemical Engineering Department, University of Granada, Avda. Fuentenueva, s/n 18071, Granada, Spain, Tel. +34 958 243315; Fax: +34 958 248992; email: alirg@ugr.es*

Received 3 February 2014; Accepted 21 June 2014

ABSTRACT

In this work, results of the biosorption of Cr^{6+} and Ni^{2+} by sugarcane bagasse in two up-flow fixed-bed columns in series have been presented. The experimental data were adjusted for several kinetic models that describe the breakthrough curve obtained for a single column and for two columns in series. The Dose–Response model is the one that better adjusts the experimental data for the studied metals with a high correlation coefficient. Although with a single column, it is possible to reduce the metal concentrations under the requirements of Cuban normative, the use of two columns in series guarantees concentration nearly to 0 for two metals. So, the percentage removal with two columns in series were 98.2 and 92.8% for Cr^{6+} and Ni^{2+}, respectively.

Keywords: Biosorption; Fixed-bed columns; Sugarcane bagasse; Heavy metals; Modeling

1. Introduction

The presence of heavy metals, such as cadmium, chromium, lead, zinc, nickel, copper, and mercury, in the environment pose a major threat in view of their bioaccumulation tendency and toxicity [1]. Hence, removal of these heavy metals from the environment is the paramount importance. Among the most common pollutant, heavy metals found in industrial effluents is chromium, and specifically, Cr^{6+} is one of the most toxic metals because of its mutagenic and carcinogenic properties to animals and humans, causing death if a few grams are ingested [2–5]. Cr^{6+} is found in electroplating, leather tanning, pulp production, metal finishing, paint, and petroleum refining wastes. Another heavy metal commonly found in industrial effluents is Ni^{2+}. It belongs to the so-called "essential" metals and is identified as a component in a number of enzymes, participating in important metabolic reactions such as ureolysis, hydrogen metabolism, methane biogenesis, and acid genesis. But Ni^{2+} ion intake over the permissible levels results in different types of disease such as pulmonary fibrosis, renal edema, skin dermatitis, and gastrointestinal distress (e.g. nausea, vomiting, diarrhea) [6]. Mining and metallurgy of nickel, stainless steel, aircraft industries, nickel electroplating, battery and manufacturing, and pigments and

*Corresponding author.

ceramic industries wastewaters contain high amounts of nickel ions [7]. So it is essential to remove these metals from wastewater before disposal. Conventional chemical processes, such as precipitation, ion exchange, chemical oxidation, and reverse osmosis, are known for the removal of these heavy metals. However, the overall process involves huge capital for its operation and is influenced by several criteria and therefore there is a need for an economic and safe approach towards remediation of heavy metals. In this regard, use of micro-organisms for the removal of heavy metals gains significance [8–11].

Biosorption uses the ability of dead/inactive biomass to remove heavy metals from aqueous solutions. The major advantages of the biosorption technology are its effectiveness in reducing the concentration of heavy metal ions to very low levels and the use of inexpensive biosorbent materials [12,13]. The utilization of agro-wastes as adsorbent is currently receiving wide attention because of their abundant availability and low cost [14,15]. In this sense, among the various agro-wastes, sugarcane bagasse seems to be an important aspirant. Sugarcane bagasse is a lignocellulose plant waste that composed approximately of 40% cellulose, 24% hemicellulose, and 25% lignin [16,17]. This composition of sugarcane bagasse gives good properties to be capable to take up metals and suggests the use of sugarcane bagasse as a low-cost natural biosorbent for heavy metals. Although nowadays, researchers are focusing on modification of biomass, such as immobilized and pretreatments of biomass, to enhance the adsorption of heavy metals; Khoramzadeh et al. [18] obtained that the chemical treatments of the sugarcane bagasse by NaOH and HCl had no significant effect on the uptake capacity. Besides, the most of authors use the sugarcane bagasse without any treatment [19,20]. So authors use the untreated biomass for the study.

Most previous researches using biosorbents for metal ions are based on batch kinetic and batch equilibrium studies. However, in the practical operation of full-scale sorption processes, continuous-flow fixed-bed columns are often chosen [21–24]. In such systems, the concentration profiles in the liquid and sorbent phases change in both space and time. From the perspective of process modeling, the dynamic behavior of a fixed-bed column is described in terms of the effluent concentration–time profile, i.e. the breakthrough curve. As a result, the development and application of predictive and simulative mathematical models for the design of continuous biosorption processes represent an important area in environmental engineering. The determination of model parameters and the verification of model validity can be obtained by well-designed laboratory-scale experiments.

2. Mathematical backgrounds

From a practical point of view, biosorption processes to great scale are carried out in a continuous way [25]. In these systems, the concentration in the liquid phase and in the solid phase varies both in space and in time due to which the design and optimization of fixed-bed columns is especially difficult if not approached through a quantitative model. In this sense, the dynamic behavior of fixed-bed columns is described in terms of “exit concentration—time,” that is to say, what is known as breakthrough. A typical breakthrough curve represents the relationship of the entry concentrations to the exit concentrations in time or the circulated volume. When the fluid passes through the column, an area of mass-transfer is defined that varies from 0% of the initial concentration (corresponding to the sorbent without solute) to 100% of the initial concentration (corresponding to the total saturation). The point where the metal concentration in the effluent reaches a certain value, generally related with the permitted limit for that metal by regulations and environmental norms, is called breakthrough point and corresponds to the breakthrough time (t_b) that allows determining the volume of treated effluent.

From a practical point of view, the saturation time (t_s) is set when the metal concentration in the effluent has a value between 90 and 95% of the initial concentration of that metal in solution. To describe the breakthrough curve, numerous models have been proposed that can be from semi-empiric simple models of few parameters that exist and easy to solve mathematically to rigorous models that consider axial dispersion in the flow direction, resistance to the film diffusion, diffusion intra matter, which can include diffusion in the surface and in the pores that generally require complicated numeric solutions [26].

These models are not only used to analyze and interpret experimental data, they also are used to predict the response of the systems when the operation conditions are changed [27].

The performance of packed-bed column is described according to the concept of the breakthrough curve that is the plot of time vs. effluent concentration:

Effluent volume is calculated from the Eq. (1):

$$V_{ef} = Q \cdot t_{total} \tag{1}$$

where t_{total}: represents the total time, (min) and Q: is the flow that circulates for the column, (mL/min).

The area under the breakthrough curve obtained by integrating the adsorbed concentration vs. time plot can be used to find the total adsorbed metal quantity. Total adsorbed metal quantity in the column for a given feed concentration and flow rate is calculated from the Eq. (2):

$$q_{\text{total}} = \frac{Q}{1,000}\int_{t=0}^{t=t_{\text{total}}} C_{\text{R}}\,\text{d}t \tag{2}$$

where C_R: is the concentration of retained metal, (mg/L).

Total amount of metal sent to column is calculated from the Eq. (3):

$$m_{\text{total}} = \frac{C_0 \cdot Q \cdot t_{\text{total}}}{1,000} \tag{3}$$

Total removal percent of metal (column performance) with respect to flow volume can also be calculated from the ratio of total quantity of metal adsorbed to the total amount of metal passed through the column, Eq. (4):

$$\%\ \text{retenido} = \frac{q_{\text{total}}}{m_{\text{total}}} \times 100 \tag{4}$$

Equilibrium metal uptake in the column is defined by Eqs. (5) and (6) as the total amount of metal sorbed per g of sorbent at the end of total flow time:

$$q_{\text{e}} = \frac{q_{\text{total}}}{m} \tag{5}$$

$$C_{\text{e}} = \frac{m_{\text{total}} - q_{\text{total}}}{V_{\text{ef}}} \times 1,000 \tag{6}$$

where m: sorbent mass used in the column, (g).

The successful design of a column adsorption process requires prediction of the concentration–time profile or breakthrough curve for the effluent.

2.1. Determination of the not used bed surface

The length of unused bed HUNB represents the mass-transfer zone. Small values of this parameter correspond to an ideal step with negligible mass-transfer resistance in the breakthrough curve. Therefore, minimum HUNB quantities are required in optimized operational conditions. The dynamic capacity of the column is defined as the amount of metal ion retained prior to the breakpoint ($C/C_0 = 5\%$). The integration of the area under the breakthrough curve gives the amount of metal not recovered by the biosorbent; based upon the difference of the quantity of metal passed through the column, this permits the determination of the amount retained by the exchanger [28,29].

The calculation of the not used bed surface obtained by the Eq. (7) constitutes a method to evaluate the capacity of biosorbents adsorption in packed columns of continuous flow.

The not used bed surface of is calculated by Eq. (7).

$$\text{SNU} = L_0\left(\frac{t_{\text{s}} - t_{\text{b}}}{t_{\text{s}}}\right) \tag{7}$$

where L_0: represents the height of the bed, (cm); t_s: represents the time at which the saturation of the bed is reached, (min); and t_b: represents the time at which the point of rupture of the bed is reached, (min).

2.2. Kinetic models

For the successful design of a column for the adsorption process, it is important to predict the breakthrough curve. Various kinetic models have been developed to predict the dynamic behavior of the column.

In this work, four models were used for kinetic studies. These models are: Adams–Bohart, Thomas, Yoon–Nelson, and Dose–Response models.

2.2.1. Adams–Bohart model

The Adams–Bohart model is used to the description of the initial part of the breakthrough curve. The Eq. (8) [30] is expressed as:

$$\text{Ln}\left(\frac{C}{C_0}\right) = K_{\text{ab}} \cdot C_0 \cdot t - \frac{K_{\text{ab}} \cdot N_0 \cdot z}{v} \tag{8}$$

The capacity removal is calculated according to the following equation:

$$q = \frac{N_0 \cdot \text{BV}_{\text{s}}}{m} = \frac{N_0}{\rho} \tag{9}$$

where K_{ab} is the kinetic constant (L/mg min), v is the linear flow rate (mL/min), Z is the bed depth of column (cm), N_0 is the saturation concentration (mg/L), t is the time (min), C_0 and C are, respectively, the adsorbate concentration at the entrance and at the exit of the column, respectively, at time t, and BV_s is the volume of the fixed bed and is the apparent density of the fixed bed.

Parameters describing the characteristic operations of the columns (K_{ab} and N_0) were calculated using linear regression analysis according to Eq. (8). From a linear plot of Ln (C/C_0) against time (t), values of K_{ab} and N_0 were determined from the intercept and slope of the plot.

2.2.2. Thomas model

The Thomas model is one of most used the theoretical models to describe the column operation, [31]. This model is described by:

$$\frac{C}{C_0} = \frac{1}{1 + e^{\left(\frac{K_{th}}{F}(q \cdot x - C_0 \cdot V_{ef})\right)}} \tag{10}$$

where C_0 and C_t are the entry and the exit concentrations respectively of the column, (mg L^{-1}), K_{th} is the Thomas constant (mL/mg min^{-1}), q is the maximum capacity of adsorption (mg g^{-1}), x is the quantity of adsorbent in the column (g), V_{ef} is the volume of the solution (mL) and F is the volumetric flow (mL min^{-1}).

The linearized Eq. (10) is:

$$\text{Ln}\left(\frac{C_0}{C} - 1\right) = \frac{K_{th} \cdot q \cdot m}{Q} - \frac{K_{th} \cdot C_0}{Q} V \tag{11}$$

Values of q and K_{th} were determined from the intercept and slope of the linear plot of $\text{Ln}\left(\frac{C_0}{C} - 1\right)$ against time (t).

2.2.3. Yoon–Nelson model

Yoon and Nelson [32] developed a model based on the assumption that the rate of decrease in the probability of adsorption of adsorbate molecule is proportional to the probability of the adsorbate adsorption and the adsorbate breakthrough on the adsorbent. The linearized Yoon–Nelson model for a single component system is expressed as:

$$-\frac{\partial A}{\partial t} = k_{YN}(t - \tau) \tag{12}$$

The linearized Yoon–Nelson model for a single component system is expressed as:

$$\text{Ln}\left(\frac{C}{C_0 - C}\right) = k_{YN}(t - \tau) \tag{13}$$

where k_{YN} (1/min) is the rate velocity constant and τ (min) is the time required for 50% adsorbate breakthrough. From a linear plot of $\text{Ln}\left(\frac{C_0}{C} - 1\right)$ against sampling time (t), values of k_{YN} and τ were determined from the intercept and slope of the plot for a given height, flow, and the initial concentration.

2.2.4. Dose–Response model

This model has been commonly used in pharmacology to describe different types of processes and it is being, at the present time, an employee for describing the biosorption processes in columns [33,34].

The general equation that represents the model is the following:

$$Y = b_0 - \frac{b_0}{1 + \left(\frac{X}{b_2}\right)^{b_1}} \tag{14}$$

where X and Y represent the dose and the response in terms of percentage of the maximum possible response, respectively. The parameter b_0 is the response when the saturation is reached, b_1 represent the slope of the function, and b_2 indicates the concentration to which 50% of the maximum response is obtained.

The Dose–Response model applied in biosorption columns is described for Eq. (15):

$$\frac{C}{C_0} = 1 - \frac{1}{1 + \left(\frac{C_i \cdot V_{ef}}{q_0 \cdot m}\right)^{a}} \tag{15}$$

This model has a relative importance as it describes the complete curve of rupture with high precision; however, it is difficult to relate the empiric parameter a with the experimental conditions for what is practically impossible for the scale change of the system [33].

3. Materials and methods

3.1. Biosorbent materials

Sugarcane bagasse samples were collected from the Sugar Power Station located in the Central University "Marta Abreu" of Las Villas, Santa Clara. The bagasse underwent a sieving process in a sieve machine Model MLW with a group of sieves (Series Tyler), the fraction between 1 and 0.5 mm being the major interest.

Fig. 1 corresponds to a sample of natural bagasse, which was subjected to a process of reduction of particle size with the purpose of improving their capacity of adsorption.

3.2. Preparation of standards and reagents

Solutions of chloride of nickel(II) and dichromate of potassium ($K_2Cr_2O_7$) were prepared at different concentrations and values of pH. The solutions of nickel chloride were prepared to 10 and 20 mg/L and those of dichromate of potassium were prepared to 10 and 15 mg/L with distilled water. To adjust the initial pH of the solutions, appropriate quantities of HCl 0.1 M were added. The initial pH of the solutions of dichromate of potassium was fixed to 2 and that of the solutions of nickel chloride were fixed to 5.

3.3. Hydraulic tests and selection of the operation parameters

Before tests of adsorption, hydraulic tests were carried out. Two columns are filled with natural sugarcane bagasse and water was circulated with the purpose of determining the most appropriate flows for the established operation conditions.

The best flow allows that the bed keeps stable, not fragment, and no-draining when the operation stops, besides being achieved a fall of appropriate pressure. The selected feeding flow is of 2 mL/min. For the selection of the height of the bed, the design approaches [27] that outline that it can be six times or more than the interior diameter of the column are taken into account.

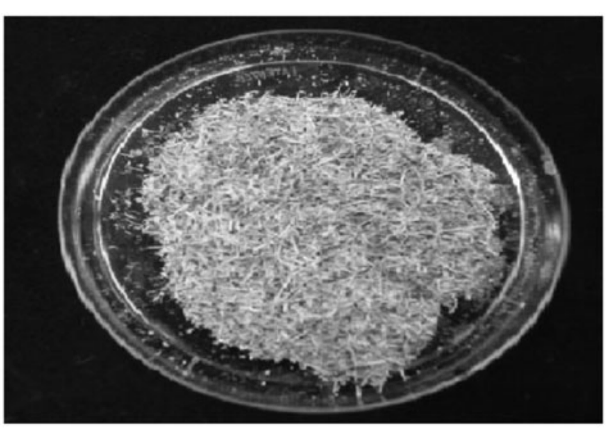

Fig. 1. Sample of natural sugarcane bagasse.

3.4. Quantification of the samples

Once studied the biosorption of Ni^{2+} and Cr^{6+} using two columns of fixed bed in series (Fig. 2), several models were applied to the experimental data of the breakthrough curves for the appropriate fitting and the determination of the parameters of those models. The main parameters were calculated by the mentioned equations that define the behavior of the process of biosorption.

During the experiments, the samples from each column were collected a frequency of 5 min for the first 100 min and then each 10 min, until achieving the saturation of the biosorbent.

The chromium and nickel concentrations were determined to determine the removal percent in each column in series using the technique of atomic absorption using Pye Unicam SP9 PHILIPS Atomic Absorption Spectrophotometer. Chromium Analytical Line: 357.9 nm.

4. Results and discussion

4.1. Results at laboratory scale of biosorption of Cr^{6+} and Ni^{2+} in fixed-bed columns with sugarcane bagasse

To analyze the dynamic Cr^{6+} and Ni^{2+} removal in two up-flow fixed-bed columns in series, breakthrough curves (C/C_0 vs. (t) time) were drawn and

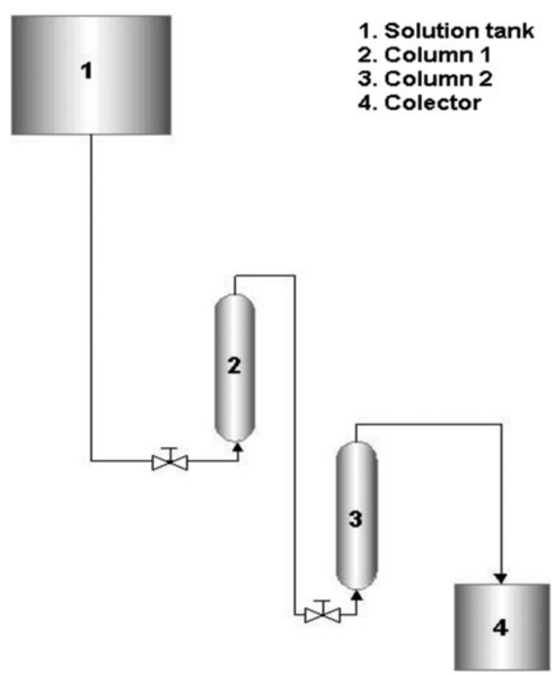

Fig. 2. Diagram of laboratory set up to remove Ni^{2+} and Cr^{6+} ions using two fixed columns in series by sugarcane bagasse.

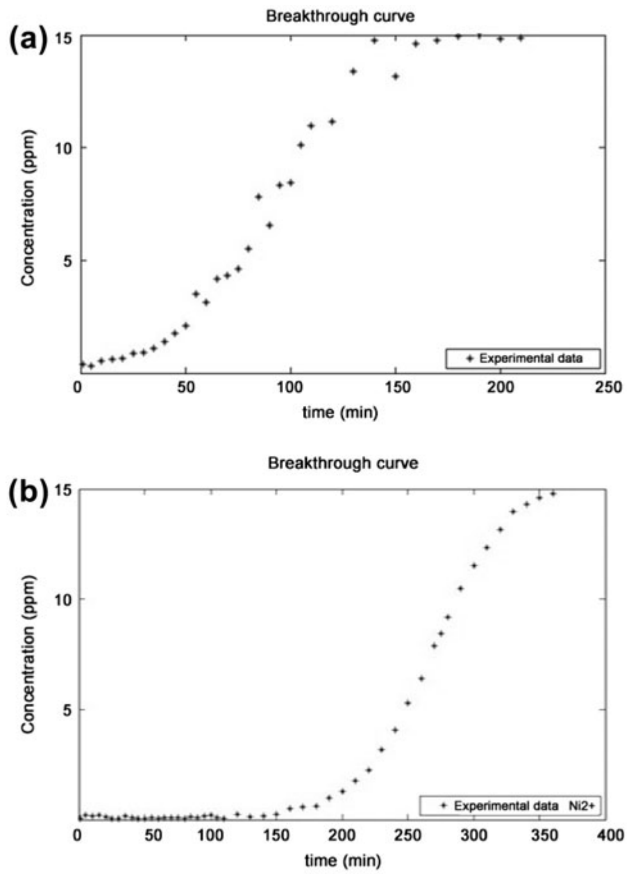

Fig. 3. Obtained breakthrough curve for the biosorption of Cr^{6+} to the exit of the first column (Fig. 3(a)) and to the exit of the second column (Fig. 3(b)) at an initial concentration of 15 mg/L and height of bed of 20 cm.

the data were evaluated with the help of the equations previously described.

4.1.1. Removal of Cr^{6+}

All the experiments were carried out at a constant temperature of 25°C and pH = 2. From the results obtained, it is determined that the best operation conditions to achieve the highest retention of Cr^{6+} are flow = 2 mL/min, C_0 = 15 mg/L, and biosorbent mass = 1.5 g (height of bed = 20 cm). The data obtained experimentally were processed with MATLAB 2007a.

Fig. 3(a) represents the breakthrough curves for the removal of Cr^{6+} from the first column of the series and Fig. 3(b), from the second column of the series.

From the experimental data of Fig. 3, the most significant parameters of the breakthrough curves [breakthrough time (t_r), total quantity of metal removal (q_{total}), total quantity of metal that passes through the column (m_{total}), biosorption capacity (q_e), and percentage of metal removal (R)] were obtained. These results are summarized in Table 1.

It is observed that, in second column, the breakthrough and saturation time are higher than in first columns. It can be due to that, in second column, the effluents entries with a lower concentration of metal. Besides, the percentage removal was also higher (nearly to 100%) in second column. On the other hand, data showed that the height not used of the column is enough high, being bigger when mass of the biosorbent increased.

Table 1
Characteristic parameters of the breakthrough curves for Cr^{6+} and Ni^{2+} in two packed columns in series with sugarcane bagasse

Metal	m_o	C_0 (mg/L)	C_1 (mg/L)	C_2 (mg/L)	L (cm)	t_{s_1} (min)	t_{s_2} (min)	t_b (min)	%Remo 1	%Remo 2	SNU 1 (cm)	SNU 2 (cm)
Cr^{6+}	1	10	1.72	0.62	15	115	290	45	82.80	93.80	9.13	12.67
	1.5	10	1.94	0.57	20	180	330	45	80.60	94.30	15.00	17.27
	1	15	1.97	0.44	15	170	210	20	86.86	97.06	13.23	13.57
	1.5	15	1.75	0.27	20	210	310	45	88.33	98.2	15.71	17.09
Ni^{2+}	1	15	2.32	0.04	15	270	360	45	84.53	99.73	12.50	13.12
	1.5	15	1.26	0.11	20	310	460	120	91.60	99.26	12.25	14.78
	1	25	1.91	0.08	15	95	250	20	92.36	99.69	11.84	13.80
	1.5	25	1.79	0.09	20	180	330	70	92.84	99.64	12.22	15.75

Notes: where m_o, the biosorbent mass; C_0, the initial concentration; C_1, the concentration in the point of rupture of first column; C_2, the concentration to the column exit 2 in the time of rupture for the first column; L, column longitude; t_{s_1}, time of saturation of the first column; t_{s_2}, time of saturation of the second column; t_b, rupture point; SNU, height of not used column.

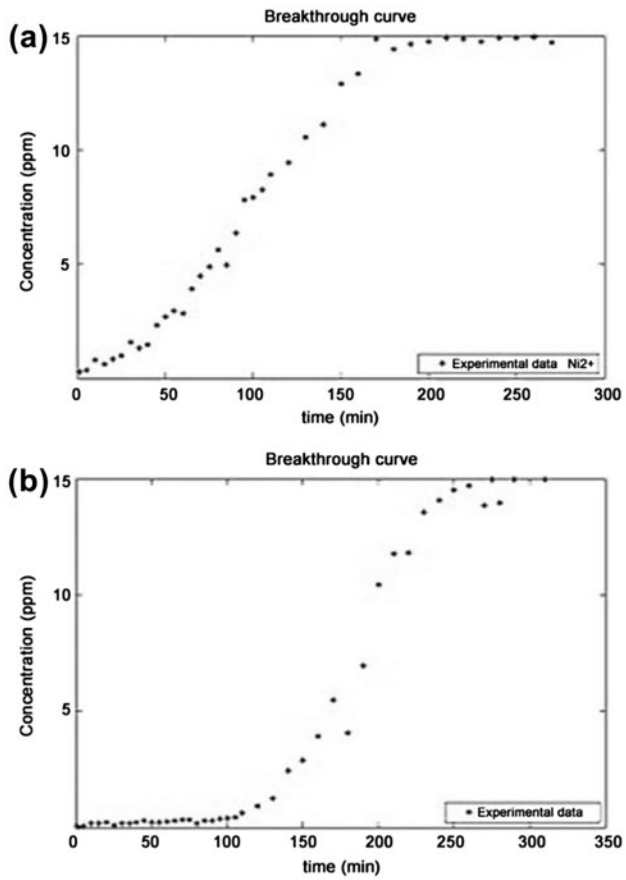

Fig. 4. Obtained breakthrough curve for the biosorption of Ni^{2+} to the exit of the first column (Fig. 4(a)) and to the exit of the second column (Fig. 4(b)) at an initial concentration of 25 mg/L and height of bed of 15 cm.

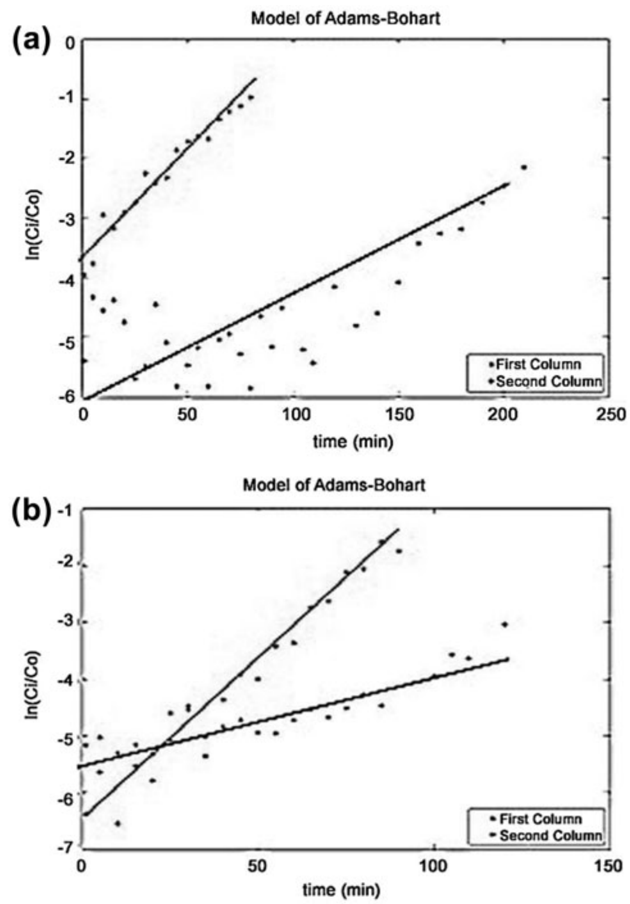

Fig. 5. Adjusts of model of Adams–Bohart with the experimental data of Cr^{6+} for the concentration of 15 mg/L and height of bed of 15 cm from the exit of first column and second column (Fig. 5(a)) and concentration of 10 mg/L and height of bed 20 cm exit from first and exit from second column (Fig. 5(b)).

4.1.2. Removal of Ni^{2+}

All the experiments were carried out at a constant temperature of 25°C and pH = 5. Similar to Cr^{6+}, according to the results obtained from the experimental design, the best operation conditions are considered where the removal percentage of the metal ion is the highest, which, in this case, are as follows: flow = 2 mL/min, C_0 = 25 mg/L, and biosorbent mass = 1.5 g (height of bed = 20 cm). The results are also reported for the following experimental conditions: flow = 2 mL/min, C_0 = 15 mg/L, and biosorbent mass = 1.5 g (height of bed = 15 cm). These experiments were carried out to corroborate the effect of the bed height. The saturation time is determined when C/C_0 is higher than 0.9, which means that exit concentration of the effluent is 90% of the initial metal concentration in the first column. The data obtained experimentally were also processed and adjusted in MATLAB 2007a.

The breakthrough curve for the removal of Ni^{2+} in first column is shown in Fig. 4(a) and for two columns in series in Fig. 4(b).

About removal of Ni(II), from the experimental data of this figure, the most significant parameters of the breakthrough curves were obtained. These results are also summarized in Table 1. The behavior of biosorption of Ni^{2+} was similar to biosorption of Cr^{6+}. However, in this metal, the difference of percentage removal between two columns was lower (10% approximately). However, the breakthrough and saturation time of second column were higher than those for the first column. The explanation is the same for Cr^{6+}, therefore, the inlet metal concentration of second column was around 7–15% of the one for first column.

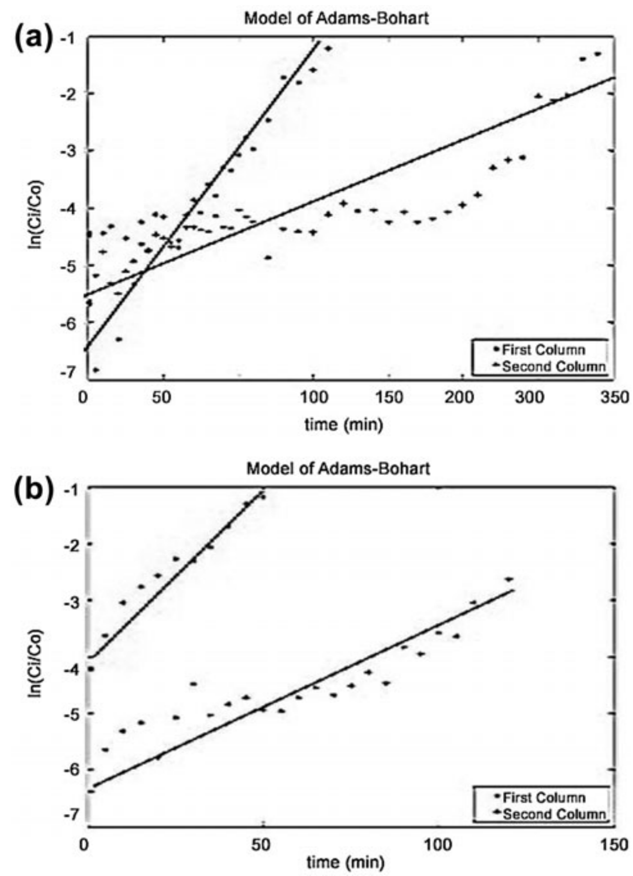

Fig. 6. Adjusts of model of Adams–Bohart with the experimental data of Ni^{2+} for the concentration of 15 mg/L and height of bed of 15 cm from the exit of first column and second column (Fig. 6(a)), and for the concentration of 25 mg/L and height of 20 cm from the exit of first and the second column (Fig. 6(b)).

4.2. Breakthrough curves: adjust of models and determination of kinetic parameters

4.2.1. Adams–Bohart model for two columns in series

In accordance with numerous authors, the Adams–Bohart model is mainly used when the concentration in the effluent is lower than 0.15 C_0 [35–37]. Therefore, the Adams–Bohart adsorption model was applied to experimental data for the description of the initial part of the breakthrough curve. Experimental breakthrough curves of Cr^{6+} obtained at inlet concentrations of 10 and 15 mg/L are shown in Fig. 5 and curves of Ni^{2+} obtained at inlet concentrations of 15 and 25 mg/L are shown in Fig. 6. The model parameters were obtained using linear regression analysis according to Eq. (8), and the results are listed in Tables 2 and 3 for Cr^{6+} and Ni^{2+}, respectively. The model does not reproduce the breakthrough curves acceptably (see the R^2 values). However, the values of the maximum volumetric sorption, N_0, increase when mass of biosorbent increased and when initial metal concentration increased. The fitted for Ni^{2+} was worse than for Cr^{6+}, with lower values of R^2. However, the trend of maximum volumetric sorption was similar (it increases with mass of biosorbent and with inlet concentration). On the other hand, the capacity of volumetric sorption does not diminish with the increase in bed height for all the cases; likewise the kinetic constant, K_{ab}, increases with the bed height that indicates that the biosorption process takes place with higher velocity. These results are similar to those obtained by other investigators [38–40].

Table 2
Adjusts of the data of removal of Cr^{6+} using a series of two packed columns with sugarcane bagasse to the models of Adams–Bohart, Thomas, Yoon–Nelson and Dose–Response

Column		Initial concentration of column 1 (mg/L)	Adams–Bohart			Thomas			Yoon–Nelson			Dose–Response		
#	Biosorbent mass (g)		R^2	K_{ab}	N_0	R^2	K_{th}	q_0	R^2	k_{YN}	τ	R^2	a	q_0
1	1	10	92.81	0.00612	22.21	92.31	4.1	1.10	92.31	0.041	55.29	95.95	3.31	1.05
2	1	10	95.26	0.00256	27.022	97.68	2.9	1.22	97.68	0.029	122.20	97.67	5.00	1.29
1	1.5	10	97.11	0.00275	46.64	96.76	3.79	1.11	96.76	0.038	83.48	97.29	4.51	1.12
2	1.5	10	99.61	0.00584	16.51	98.14	2.59	1.11	98.14	0.026	166.56	97.09	4.43	1.11
1	1	15	79.51	0.00144	129.90	92.28	2.43	1.93	92.28	0.0365	64.36	92.075	2.73	1.78
2	1	15	79.90	0.00213	116.92	96.59	3.00	2.09	96.59	0.045	104.62	99.43	5.06	1.83
1	1.5	15	96.94	0.00242	118.56	97.43	3.2	1.72	97.43	0.048	86.45	99.21	4.36	1.75
2	1.5	15	79.24	0.00131	229.04	93.09	2.44	1.72	93.09	0.0367	172.72	98.65	8.77	1.86

Table 3
Adjusts of the data of removal of Ni^{2+} using a series of two packed columns with sugarcane bagasse to the models of Adams–Bohart, Thomas, Yoon–Nelson and Dose–Response

Column		Initial concentration of column 1 (mg/L)	Adams–Bohart			Thomas			Yoon–Nelson			Dose–Response		
#	Biosorbent mass (g)		R^2	K_{ab}	N_0	R^2	K_{th}	q_0	R^2	k_{YN}	τ	R^2	a	q_0
1	1	15	95.62	0.002340	117.07	95.96	2.33	2.95	95.96	0.035	98.65	97.64	2.95	2.33
2	1	15	72.93	0.001050	423.00	89.21	1.76	3.96	89.21	0.029	264.34	99.7	10.1	3.98
1	1.5	15	82.00	0.00174	183.07	96.42	2.41	3.42	96.42	0.0362	171.38	99.48	7.71	3.52
2	1.5	15	75.42	0.000500	274.60	80.67	1.13	3.66	80.67	0.017	366.17	99.54	15.2	3.66
1	1	25	91.79	0.002248	129.25	94.06	1.60	4.33	94.06	0.0402	86.64	98.45	4.11	3.11
2	1	25	85.00	0.00088	251.03	92.90	1.76	4.01	92.90	0.044	160.40	99.58	9.77	3.90
1	1.5	25	89.64	0.001960	175.92	96.70	2.28	3.74	96.70	0.057	112.15	98.41	5.99	3.60
2	1.5	25	79.24	0.000500	331.51	76.58	1.40	4.03	76.58	0.035	241.75	99.21	15.3	4.14

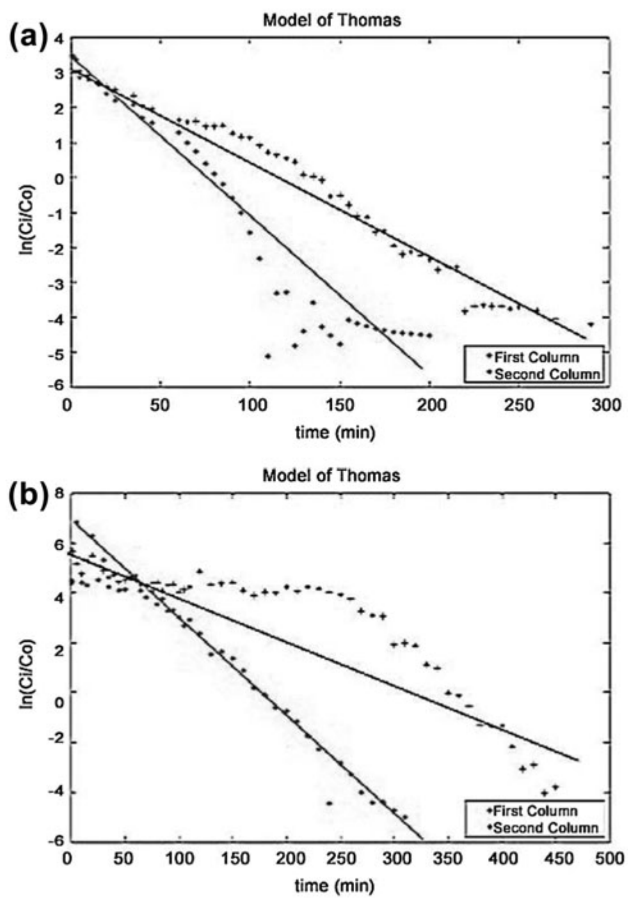

Fig. 7. Adjusts of Thomas model with the experimental data of Cr^{6+} for the concentration of 10 mg/L and height of bed of 15 cm to the exit of first column and second column (Fig. 9(a)), and for the concentration of 15 mg/L and height of 20 cm to the exit of first and to the exit of second column (Fig. 9(b)).

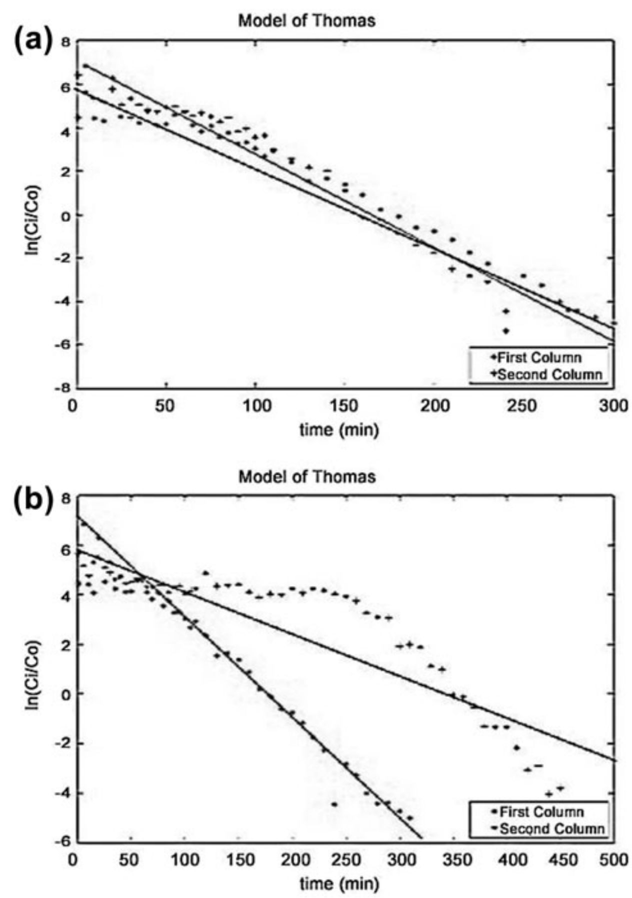

Fig. 8. Adjusts of Thomas model with the experimental data of Ni^{2+} for the concentration of 25 mg/L and height of bed of 15 cm from the exit of first column and second column (Fig. 10(a)), and for the concentration of 15 mg/L and height of 15 cm to the exit from first and to the exit of second column (Fig. 10(b)).

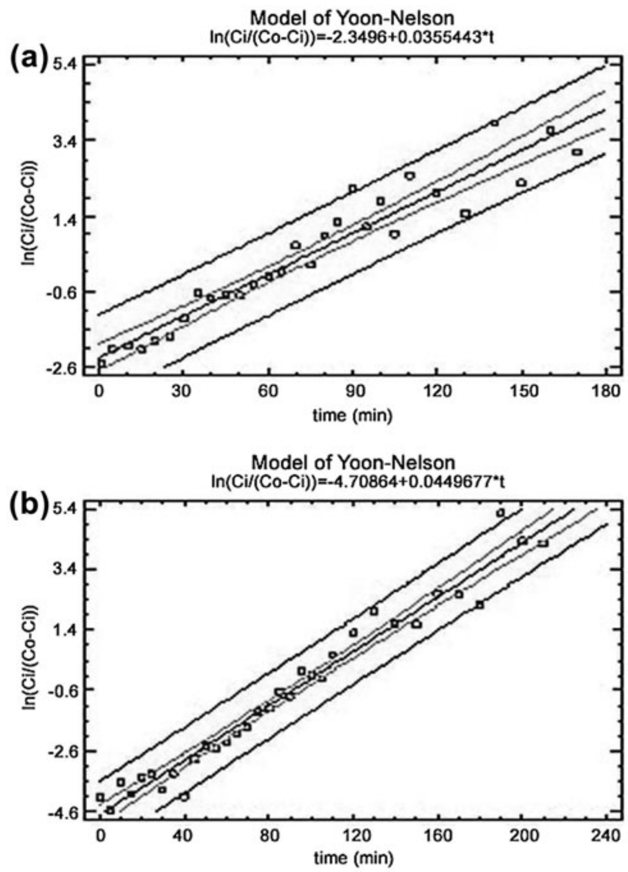

Fig. 9. Adjusts of model of Yoon–Nelson with the experimental data of Cr^{6+} for the concentration of 10 mg/L and height of bed of 15 cm to the exit of first column (Fig. 7(a)) and to the exit of second column (Fig. 7(b)).

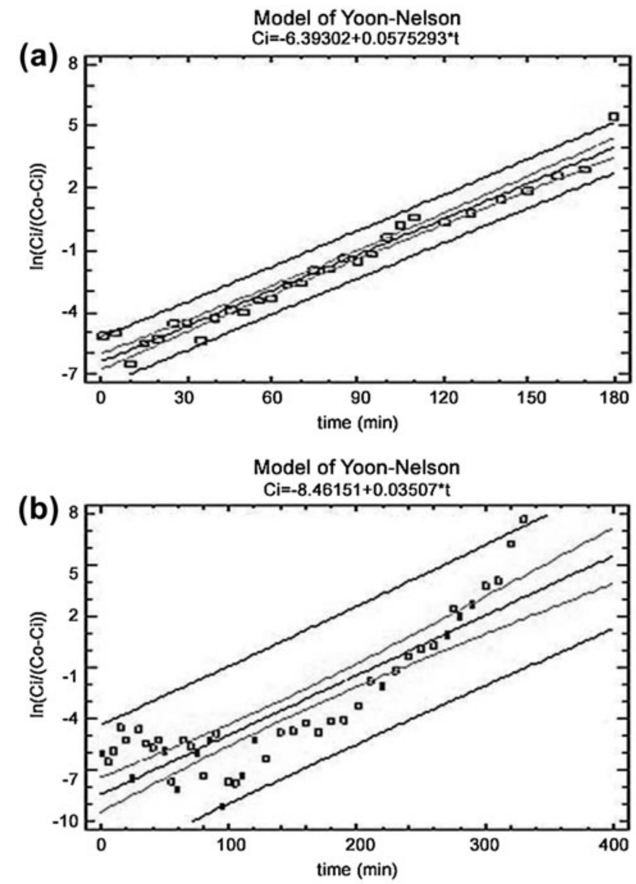

Fig. 10. Adjusts of model of Yoon–Nelson with the experimental data of Ni^{2+} for the concentration of 25 mg/L and height of bed of 15 cm to the exit of first column (Fig. 8(a)) and to the exit of second column (Fig. 8(b)).

4.2.2. *Thomas model for two columns in series*

This model is one of the most used to describe the behavior of the biosorption process in fixed-bed columns. The model parameters were obtained according to Eq. (11) using linear regression analysis. They are shown in Tables 2 and 3 for each concentration and for each used bed heights for Cr^{6+} and Ni^{2+}, respectively. It was observed that obtained values of q_0 increased with the initial metal concentration.

This model has been applied between the breakthrough time and the saturation time in the column. Thomas model best reproduces the experimental results for all the cases, with close similarity between the experimental and the calculated values, as shown in Figs. 7(a), (b), 8(a), and (b), with high values of R^2.

Several research works report the application of Thomas model with different results. In this context, Vázquez et al. [41], studying the optimization of the biosorption of lead, copper and, zinc with chestnut shell, indicates that Thomas model does not reproduce the breakthrough curve in an acceptable way due to differences between the experimental and calculated retention capacity.

Han et al. [42], studied the copper adsorption in column of fixed-bed using a recovered zeolite of iron oxide and it is indicated that Thomas model reproduces the breakthrough curve being obtained and that the q_0 values are practically independent of the height of used bed and different to those obtained experimentally. Mata et al. [43], found that Thomas model reproduces the breakthrough curves in an acceptable way.

4.2.3. *Yoon–Nelson model for two columns in series*

The model of Yoon–Nelson is mathematically equivalent to model of Thomas. Starting from the Eq. (13) and by means of lineal regression using the

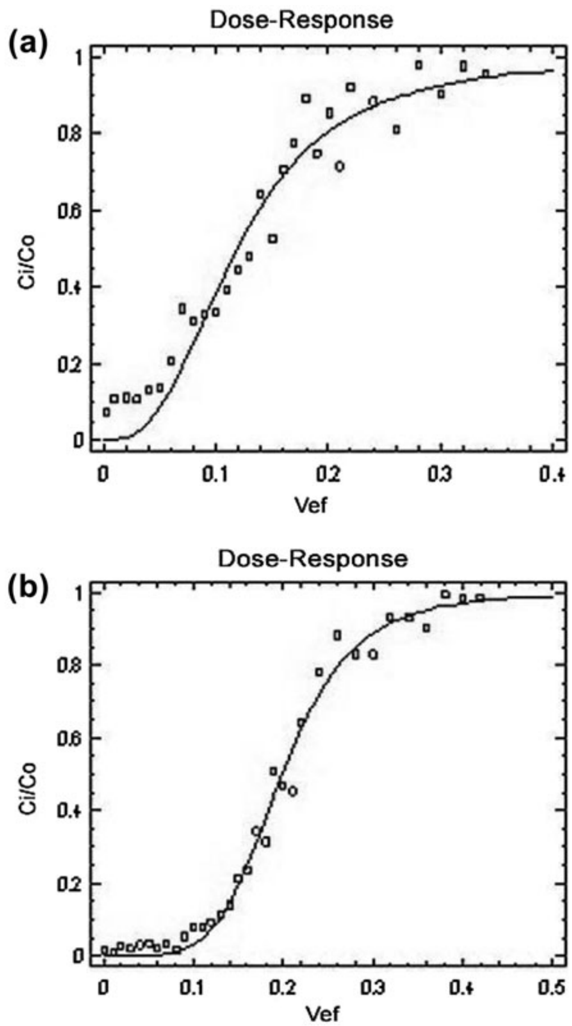

Fig. 11. Adjusts of model of Dose–Response with the experimental data of Cr^{6+} for the concentration of 15 mg/L and height of bed of 15 cm to the exit from first column (Fig. 11(a)) and to the exit from second column (Fig. 11(b))

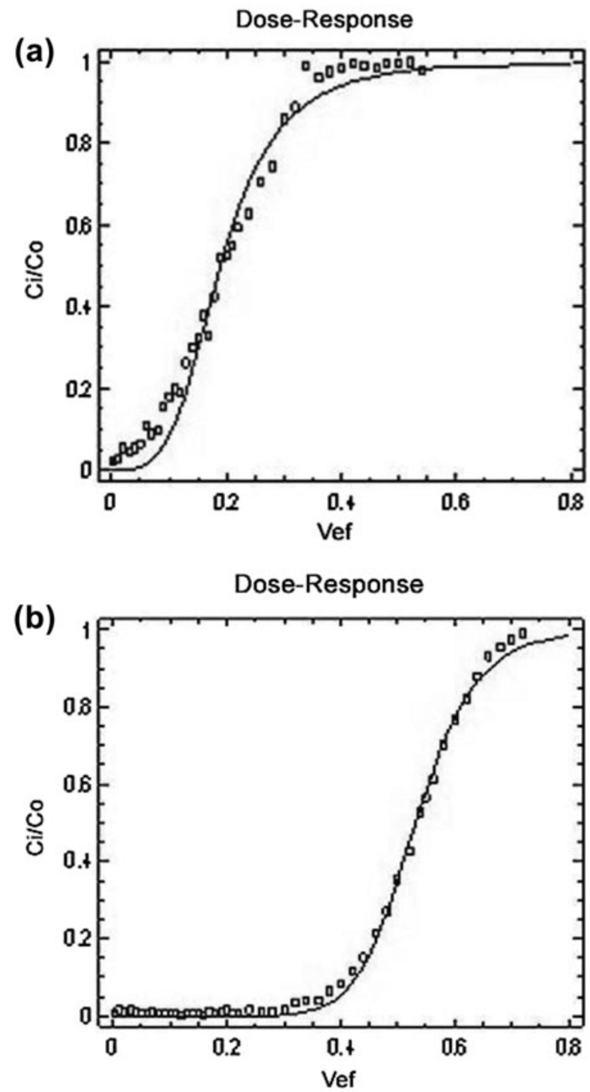

Fig. 12. Adjusts of model of Dose–Response with the experimental data of Ni^{2+} for the concentration of 15 mg/L and height of bed of 15 cm to the exit from first column (Fig. 12(a)) and to the exit from second column (Fig. 12(b)).

programming in MATLAB2007a, the parameters of the model is obtained and fitted as shown in Tables 2 and 3 for each one of the metals and with each one of the used bed heights. The Yoon–Nelson model also fitted well to the breakthrough curves obtained for the sorption of Cr^{6+} and Ni^{2+} in a packed column under different experimental conditions (Tables 2 and 3 respectively). This model is mathematically similar to that of Thomas one, so it reproduces the experimental results same way as shown in Figs. 9(a), (b), 10(a), and (b). Nevertheless, the values of the time required to retain 50% of the initial metal, τ, are very similar to those obtained experimentally, which coincides with that reported by diverse researchers for different systems biosorbent metal in bed column [44,45].

4.2.4. Dose–Response model for two columns in series

Using Eq. (15) and through non-lineal regression using MATLAB2007a, the parameters of Dose–Response models are obtained and fitted, as shown in Tables 2 and 3 for each metals and with each bed heights under study.

The results show that this model reproduces the breakthrough curves in an acceptable way, Figs. 11(a), (b), 12(a), and (b), for the studied metals and for the two bed heights under study (values of $R^2 > 0.90$). Nevertheless, as it has been indicated previously, this model reproduces the complete breakthrough curves quite well in general, but in some cases, it is difficult to

Table 4
Comparison of Cr^{6+} and Ni^{2+} biosorption capacity of sugarcane bagasse with that of different biomasses

Metal	Sorbent	q (mg/g)	Ref.
Ni^{2+}	Waste of tea factory	11.1	[48]
	Sphagnum peat moss	5.41	[49]
	Mollusk shells	0.33	[49]
	Calcium-treated anaerobic biomass	15	[50]
	Grape stalk wastes	14	[51]
	Sugarcane bagasse	4.14	This work
Cr^{6+}	Soya cake	0.28	[52]
	Chinese reed	1.85	[53]
	Turkish brown coals	0.6	[54]
	Olive stone	5.2	[55]
	Sugarcane bagasse	1.86	This work

relate the adjustment parameters with the operation conditions due to which, it has been found to have little utility to model the behavior of the column and therefore for the scale up of the same. These results are similar to those obtained by other investigators [25,46,47].

Obtained results in this work were compared in Table 4 with results obtained by other authors for these metals.

5. Conclusions

The experiments were carried out to laboratory scale using two fixed-bed columns in series with sugarcane bagasse and results showed that the biosorption is adequately alternative to remove Cr^{6+} and Ni^{2+} from aqueous solutions by the sugarcane bagasse in fixed beds. The effluent concentration of the first column meets the requirements of Cuban Normative NC 27, 2012, for Ni^{2+} and Cr^{6+} in wastewater effluent; however, the series of two columns guarantees that the concentration of these metals is close to zero for each heavy metal studied. Obtained data indicated that to remove Cr^{6+}, the best operation conditions were obtained for a bed height of 20 cm and an initial concentration of 15 mg/L. Under these conditions, in the first column, the percentage removal was 88.33%, while with two columns in series, this percentage increased to 98.2% retained. For solutions of Ni^{2+}, the best conditions were obtained for a bed height of 20 cm and an initial concentration of 25 mg/L, obtaining percentages of removal of 92.84 and 99.64% for one column and for two columns in series, respectively.

References

[1] A. Bhatnagar, A.K. Minocha, M. Sillanpää, Adsorptive removal of cobalt from aqueous solution by utilizing lemon peel as biosorbent, Biochem. Eng. J. 48 (2010) 181–186.

[2] V.K. Singh, P.N. Tiwari, Removal and recovery of chromium(VI) from industrial waste water, J. Chem. Technol. Biotechnol. 69 (1997) 376–382.

[3] N.K. Hamadi, X.D. Chen, M.M. Farid, M.G.Q. Lu, Adsorption kinetics for the removal of chromium(VI) from aqueous solution by adsorbents derived from used tyres and sawdust, Chem. Eng. J. 84 (2001) 95–105.

[4] E. Demirbas, M. Kobya, E. Senturk, T. Ozkan, Adsorption kinetics for the removal of chromium(VI) from aqueous solutions on the activated carbons prepared from agricultural wastes, Water SA 30 (2004) 533–539.

[5] D. Park, Y.S. Yun, J.M. Park, Reduction of hexavalent chromium with the brown seaweed *Ecklonia* biomass, Environ. Sci. Technol. 38 (2004) 4860–4864.

[6] N. Akhtar, J. Iqbal, M. Iqbal, Removal and recovery of nickel(II) from aqueous solution by loofa sponge-immobilized biomass of *Chlorella sorokiniana*: Characterization studies, J. Hazard. Mater. 108 (2004) 85–94.

[7] A. Özer, G. Gürbüz, A. Çalimli, B.K.J. Körbahti, Investigation of nickel(II) biosorption on *Enteromorpha prolifera*: Optimization using response surface analysis, J. Hazard. Mater. 152 (2008) 778–788.

[8] D.R. Lovley, J.R. Lloyd, Microbes with a mettle for bioremediation, Nat. Biotechnol. 18 (2000) 600–601.

[9] K. Vijayaraghavan, T.T. Teo, R. Balasubramanian, U.M. Joshi, Application of *Sargassum* biomass to remove heavy metal ions from synthetic multi-metal solutions and urban storm water runoff, J. Hazard. Mater. 164 (2009) 1019–1023.

[10] K. Vijayaraghavan, R. Balasubramanian, A comparative evaluation of sorbents for the treatment of complex metal-bearing laboratory wastewaters, J. Environ. Chem. Eng. 1 (2013) 473–479.

[11] I. Ali, V.K. Gupta, Advances in water treatment by adsorption technology, Nat. London 1 (2006) 2661–2667.

[12] J.P.K. Wong, Y.S. Wong, N.F.Y. Tam, Nickel biosorption by two chlorella species, *C. vulgaris* (a commercial species) and *C. miniata* (a local isolate), Bioresour. Technol. 73 (2000) 133–137.

[13] I. Ali, The quest for active carbon adsorbent substitutes: Inexpensive adsorbents for toxic metal ions removal from wastewater, Sep. Purif. Rev. 39 (2010) 95–171.
[14] I. Ali, New generation adsorbents for water treatment, Chem. Rev. 112 (2012) 5073–5091.
[15] I. Ali, M. Asim, T.A. Khan, Low cost adsorbents for the removal of organic pollutants from wastewater, J. Environ. Manage. 113 (2012) 170–183.
[16] S. Ho Lee, C. Hun Jung, H. Chung, M. Yeal Lee, J.W. Yang, Removal of heavy metals from aqueous solution by apple residues, Process Biochem. 33 (1998) 205–211.
[17] R.E. Treybal, Operaciones de Transferencia de Masa, Ediciones Revolución, La Habana, 1980.
[18] E. Khoramzadeh, B. Nasernejad, R. Halladj, Mercury biosorption from aqueous solutions by sugarcane bagasse, J. Taiwan Inst. Chem. Eng. 44 (2013) 266–269.
[19] I. Alomá, M.A. Martín-Lara, I.L. Rodríguez, G. Blázquez, C. Calero, Removal of nickel(II) ions from aqueous solutions by biosorption of sugarcane bagasse, J. Taiwan Inst. Chem. Eng. 43 (2013) 275–281.
[20] C. Liu, H.H. Ngo, W. Guo, K.-L. Tung, Optimal conditions for preparation of banana peels, sugarcane bagasse and watermelon rind in removing copper from water, Bioresour. Technol. 119 (2012) 349–354.
[21] K. Vijayaraghavan, J. Jegan, K. Palanivelu, M. Velan, Batch and column removal of copper from aqueous solution using a brown marine alga *Turbinaria ornata*, Chem. Eng. J. 106 (2005) 177–184.
[22] M. Calero, F. Hernáinz, G. Blázquez, M.A. Martín-Lara, G. Tenorio, Equilibrium modelling of Cr(VI) biosorption by olive stone, in: M. Zamorano, V. Popov, A. Kungolos, C.A. Brebbia, H. Itoh (Eds.), Waste Management and the Environment IV, WIT, Boston, 2008, pp. 827–836.
[23] M. Calero, F. Hernáinz, G. Blázquez, G. Tenorio, M.A. Martín-Lara, Study of Cr(III) biosorption in a fixed-bed column, J. Hazard. Mater. 171 (2009) 886–893.
[24] I. Ali, Water treatment by adsorption columns: Evaluation at ground level, Sep. Purif. Rev. 43 (2014) 175–205.
[25] K. Vijayaraghavan, D. Prabu, Potential of *Sargassum wightii* biomass for copper(II) removal from aqueous solutions: Application of different mathematical models to batch and continuous biosorption data, J. Hazard. Mater. 137 (2006) 558–564.
[26] K.H. Chu, Prediction of two-metal biosorption equilibria using a neural network, Eur. J. Miner. Process. Environ. Prot. 3 (2003) 119–127.
[27] D. Kratochvil, A study of the metal biosorption process utilizing *Sargassum* seaweed biomass, PhD, Montreal University, 1997.
[28] E. Valdman, L. Erijman, F.L.P. Pessoa, S.G.F. Leite, Continuous biosorption of Cu and Zn by immobilized waste biomass *Sargassum* sp., Process Biochem. 36 (2001) 869–873.
[29] G. Tenorio, Caracterización de la biosorción de cromo con hueso de aceituna, PhD, Universidad de Granada, España, 2006.
[30] G. Bohart, E.Q. Adams, Some aspects of the behavior of charcoal with respect to chlorine. 1, J. Am. Chem. Soc. 42 (1920) 523–544.
[31] H.C. Thomas, Heterogeneous ion exchange in a flowing system, J. Am. Chem. Soc. 66 (1944) 1466–1664.
[32] Y.H. Yoon, J.H. Nelson, Application of gas adsorption kinetics I. A theoretical model for respirator cartridge service life, Am. Ind. Hyg. Assoc. J. 45 (1984) 509–516.
[33] G.Y.V.T. Yan, T. Viraraghavan, A new model for heavy metal removal in a biosorption column, Adsorpt. Sci. Technol. 19 (2001) 25–43.
[34] R.V.K. Senthilkumar, K. Vijayaraghavan, M. Thilakavathi, P. Iyer, Seaweeds for the remediation of wastewaters contaminated with zinc(II) ions, J. Hazard. Mater. 136 (2006) 791–799.
[35] Z. Aksu, F. Gönen, Biosorption of phenol by immobilized activated sludge in a continuous packed bed: Prediction of breakthrough curves, Process Biochem. 39 (2004) 599–613.
[36] Y. Sağ, Y. Aktay, Application of equilibrium and mass transfer models to dynamic removal of Cr(VI) ions by chitin in packed column reactor, Process Biochem. 36 (2001) 1187–1197.
[37] X. Liao, M. Zhang, B. Shi, Collagen-fiber-immobilized tannins and their adsorption of Au(III), Ind. Eng. Chem. Res. 43 (2004) 2222–2227.
[38] R. Han, J. Zhang, W. Zou, H. Xiao, J. Shi, H. Liu, Biosorption of copper(II) and lead(II) from aqueous solution by chaff in a fixed-bed column, J. Hazard. Mater. 133 (2006) 262–268.
[39] K. Pakshirajan, T. Swaminathan, Biosorption of copper and cadmium in packed bed columns with live immobilized fungal biomass of *Phanerochaete chrysosporium*, Appl. Biochem. Biotechnol. 157 (2009) 159–173.
[40] B. Saha, C. Orvig, Biosorbents for hexavalent chromium elimination from industrial and municipal effluents, Coord. Chem. Rev. 254 (2010) 2959–2972.
[41] G. Vázquez, M. Calvo, M. Sonia Freire, J. González-Alvarez, G. Antorrena, Chestnut shell as heavy metal adsorbent: Optimization study of lead, copper and zinc cations removal, J. Hazard. Mater. 172 (2009) 1402–1414.
[42] R. Han, L. Zou, X. Zhao, Y. Xu, F. Xu, Y. Li, Y. Wang, Characterization and properties of iron oxide-coated zeolite as adsorbent for removal of copper(II) from solution in fixed bed column, Chem. Eng. J. 149 (2009) 123–131.
[43] Y.N. Mata, M.L. Blázquez, A. Ballester, F. González, J.A. Muñoz, Sugar-beet pulp pectin gels as biosorbent for heavy metals: Preparation and determination of biosorption and desorption characteristics, Chem. Eng. J. 150 (2009) 289–301.
[44] M. Calero de Hoces, G. Blázquez García, A. Gálvez, M.A. Martín-Lara, Effect of the acid treatment of olive stone on the biosorption of lead in a packed-bed column, Ind. Eng. Chem. Res. 49 (2010) 12587–12595.
[45] A. Singh, D. Kumar, J.P. Gaur, Continuous metal removal from solution and industrial effluents using *Spirogyra* biomass-packed column reactor, Water Res. 46 (2012) 779–788.
[46] K. Vijayaraghavan, Y.S. Yun, Bacterial biosorbents and biosorption, Biotechnol. Adv. 26 (2008) 266–291.
[47] P. SenthilKumar, S. Ramalingam, V. Sathyaselvabala, S.D. Kirupha, S. Sivanesan, Removal of copper(II) ions from aqueous solution by adsorption using cashew nut shell, Desalination 266 (2011) 63–71.

[48] E. Malkoc, Y. Nuhoglu, Removal of Ni(II) ions from aqueous solutions using waste of tea factory: Adsorption on a fixed-bed column, J. Hazard. Mater. 135 (2006) 328–336.
[49] C. Li, P. Champagne, Fixed-bed column study for the removal of cadmium(II) and nickel(II) ions from aqueous solutions using peat and mollusk shells, J. Hazard. Mater. 171 (2009) 872–878.
[50] A.H. Hawari, C.N. Mulligan, Heavy metals uptake mechanisms in a fixed-bed column by calcium-treated anaerobic biomass, Process Biochem. 41 (2006) 187–198.
[51] C. Valderrama, J. Arévalo, I. Casas, M. Martínez, N. Miralles, A. Florido, Modelling of the Ni(II) removal from aqueous solutions onto grape stalk wastes in fixed-bed column, J. Hazard. Mater. 174 (2010) 144–150.
[52] H.M.F. Freundlich, Over the adsorption in solution, J. Phys. Chem. 57 (1906) 385–470.
[53] C. Namasivayam, W.H. Höll, Chromium(III) removal in tannery waste waters using chinese reed (*Miscanthus sinensis*), a fast growing plant, Holz Roh. Werkst. 62 (2004) 74–80.
[54] F. Gode, E. Pehlivan, Adsorption of Cr(III) ions by Turkish brown coals, Fuel Process. Technol. 86 (2005) 875–884.
[55] G. Blázquez, M. Calero, F. Hernáinz, G. Tenorio, M.A. Martín-Lara, Batch and continuous packed column studies of chromium(III) biosorption by olive stone, Environ. Prog. Sust. Energy 30 (2011) 576–585.